Transient FEM Computation of Radial Force and Torque for Bearingless Wound-Rotor Induction Motors

Jumei Cai and Gerhard Henneberger
Aachen Institute of Technology (RWTH Aachen), Department of Electrical Machines
Schinkelstraße 4, D-52056 Aachen, Germany
E-mail: caijumei@iem.rwth-aachen.de, henneberger@rwth-aachen.de

Abstract- **This paper presents a bearingless wound-rotor induction motor. The transient responses of radial force and torque in bearingless induction motors are computed with the transient finite element method (FEM) with rotating machine models. It is shown that a steady radial force to support the shaft weight and a constant torque independent of the bearing currents can be generated at the same time. The bearingless wound-rotor induction motor is compared to the bearingless squirrel cage induction motor with respect to the transient responses of radial force and torque. A control system is proposed to implement the combination of levitation and rotation.**

Keywords- bearingless motor, finite element method, levitation control, radial force.

I. Introduction

In comparison to mechanic bearings magnetic bearings can be used in driving systems where abrasion and friction are not desirable. But magnetic bearings lead to a longer shaft of the overall driving system. A better alternative are bearingless machines which combine the magnetic bearings and the driving parts of the motors in one unit. Bearingless motors can not only generate torque to drive the load but also generate a radial force to levitate the shaft. So they have the advantages of simple construction and short shaft length for the overall system. Thus, bearingless motors can be used in many industrial applications, for example, in fields of medicine and in the production of semiconductor.

Principally the bearingless conception can be implemented with induction motors, permanent magnet motors or reluctance motors. These implementations are based on the same principle but have a different rotor structure. Several works on bearingless induction motors, bearingless permanent magnet synchronous motors and bearingless reluctance motors have been reported in [1], [2], [3]. A bearingless induction squirrel cage motor has been developed at the department of electrical machines, RWTH Aachen [4].

In the bearingless squirrel cage induction motor it was found that there is a great reaction from the bearing currents to the driving performance. In order to reduce this reaction in the present work the principle of bearingless induction motors is studied from the point of view of the electromagnetic fields, and a bearingless wound-rotor induction motor is developed. The transient finite element method (FEM) is used to compute the transient responses of the radial force and the torque for rotating machines.

II. Principle

The basic principle of bearingless machines is explained in [1], [2], [3]. In principle the generation of radial force in bearingless machines is based on the asymmetrical distribution of the electromagnetic field. The superposition of two fields with different numbers of pole pairs p_1 and p_2 results in a radial force, if $p_1=p_2\pm1$ is valid. In bearingless machines it is important that the driving performance is not affected by the levitation performance. Then in induction motors the induced rotor currents should not influence the bearing field, so that the bearing field contributes only to the levitation. Hence, a bearingless induction motor with a wound-rotor which has the same number of pole pairs as the driving windings is proposed.

Fig. 1 shows the configuration of this bearingless wound-rotor induction motor. The driving windings and the rotor windings have 4 poles and the bearing windings have 2 poles. The bearing windings and driving windings are supplied with currents of the same frequency, so that a constant radial force can be generated to support the shaft weight. At the same time, the rotating field generated from the bearing windings and the rotating field generated from the driving windings have a different speed. The rotor field generated from the induced rotor currents is symmetrically distributed and rotates at the same speed as the driving field does. Therefore, it enforces the building of the radial force. Moreover, the torque can be generated only from the interaction of the 4-pole driving field and the induced 4-pole rotor

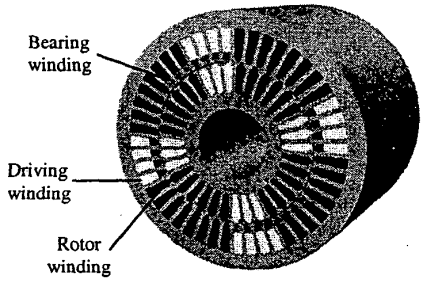

Fig. 1. Bearingless wound-rotor induction motor

currents. The bearing field does not contribute to the steady torque because the rotor field has a different number of pole pairs compared to the bearing field.

III. Transient FEM Computation Of Radial Force And Torque

A. *Transient Finite Element Method*

For the computation of radial force and torque an object oriented software package using the transient finite element method has been developed at the department of electrical machines, RWTH Aachen. Using this software package two-dimensional machine models with rotating rotor can be built and the corresponding transient responses of radial force and torque can be computed using a vector potential approach to solve the electromagnetic field.

According to Maxwell's equations the electromagnetic field in induction machines can be expressed as:

$$div\vec{B} = 0 \tag{1}$$

$$rot\vec{H} = \vec{J} \tag{2}$$

where

$\vec{B}$ is the magnetic flux density,
$\vec{H}$ is the magnetic field strength,
$\vec{J}$ is the current density.

In (1) the magnetic flux density $\vec{B}$ satisfies a zero divergence condition, it can be expressed in terms of a magnetic vector potential $\vec{A}$ as:

$$\vec{B} = rot\vec{A} \Rightarrow div\vec{B} = 0 \tag{3}$$

where

$\vec{A}$ is the magnetic vector potential.

Since the currents in bearingless induction machines flow parallel to the z axis, there will be only one component of $\vec{A}$ involved, namely A_Z, and this equation will depend on x and y only. So it is sufficient to use a two-dimensional machine model to solve the electromagnetic field. Under consideration of the iron length in the computation the results are valid for the real three-dimensional machine. Fig. 2 shows the transient vector potential distribution as a result of the FEM computation.

The peculiarity in bearingless machines is the combination of driving with levitation by itself at the same time. In addition, the fields in induction machines are rotating fields, which can not be simulated from a stationary computation. Hence, it is necessary to simulate this process using transient computation with a rotating rotor. With the transient finite element method the radial force and torque can be computed with the variation of the time and the rotor position.

The method to implement the transient FEM computation and the differences between the transient and quasi-stationary FEM has been explained in detail in [5].

Fig. 2 (a) and (b) show the transient vector potential distribution at different rotor positions according to the corresponding time variation. It is obvious that the superimposed field in the machine is a rotating field and that it is asymmetrically distributed.

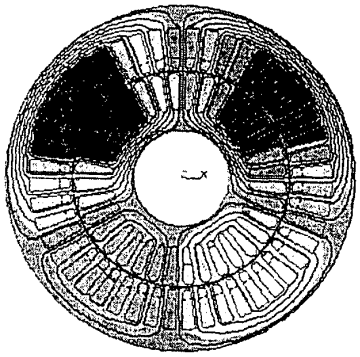

(a)

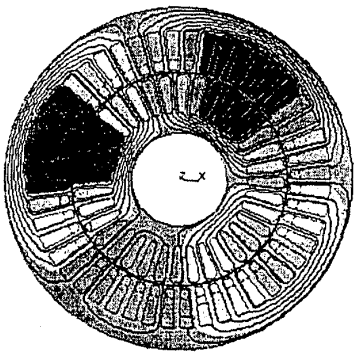

(b)

Fig. 2. Transient vector potential distribution at different rotor positions (a) and (b)

B. *Radial Force*

The radial force can be calculated from the Maxwell's stress tensor according to,

$$\vec{F} = \nu \oint_S \overline{T} \cdot \vec{n}_s \, dS \tag{4}$$

where

$\overline{T}$ is the Maxwell's stress tensor,
S is the integral area,
$\vec{n}_s$ $=(n_x, n_y)^T$, the normal vector on S,
ν $=1/\mu_0$, and
μ_0 is the permeability of air.

The Maxwell's stress tensor $\overline{T}$ in bearingless induction machines can be expressed as a two-dimensional matrix in form of the magnetic flux density in x and y direction, namely B_x and B_y as:

$$\overline{T} = \begin{bmatrix} \frac{1}{2}(B_x^2 - B_y^2) & B_x B_y \\ B_x B_y & \frac{1}{2}(B_y^2 - B_x^2) \end{bmatrix} \tag{5}$$

From (4) and (5) the radial force in x and y directions, namely F_x and F_y, can be expressed as:

$$\begin{pmatrix} F_x \\ F_y \end{pmatrix} = \nu \oint_S \begin{pmatrix} \frac{1}{2}(B_x^2 - B_y^2)n_x + B_x B_y n_y \\ B_x B_y n_x + \frac{1}{2}(B_y^2 - B_x^2)n_y \end{pmatrix} dS \qquad (6)$$

From (6) we can see, that the value of the radial force depends on the asymmetry of the distribution of the flux density.

C. *Torque*

With the finite element method the torque of the bearingless induction machine can be calculated also from the Maxwell's stress tensor as:

$$\vec{M} = \oint_S \vec{r} \times d\vec{F} = \oint_S \vec{r} \times (\vec{T} \cdot \vec{n}_S)\, dS \qquad (7)$$

where

$\vec{M}$ is the torque,

$\vec{r}$ is the radius vector.

For the two-dimensional machine model $\vec{M}$ has only one component with respect to z axis, namely M_z.

IV. Comparison To The Squirrel Cage Motor

A. *Radial Force*

In bearingless induction motors the two different rotor structures, i.e. the squirrel cage rotor and the wound-rotor with 4-pole windings, result in a large difference of the radial force. Fig. 3 shows the comparison of the transient responses of the radial force from the transient FEM computation between these two different rotors. At t=0s, the driving windings are connected with driving currents. And there is no radial force. At t=0.1s, the bearing windings are connected with bearing currents, a radial force is generated.

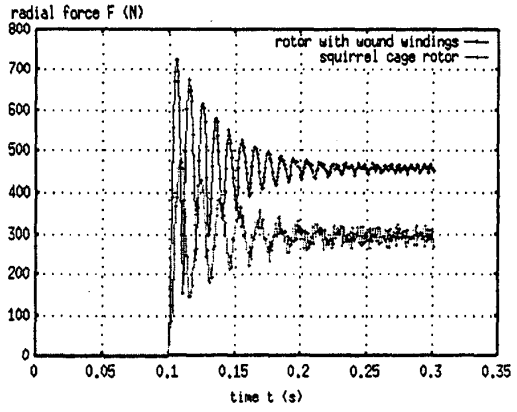

Fig. 3. Transient responses of the radial force

In bearingless induction motors with squirrel cage rotor the induced rotor currents can generate not only a 4-pole field like the driving field but also a 2-pole field like the bearing field. The superposition of these two rotor fields results in an asymmetrically distributed field, which is trying to compensate the asymmetry from the driving field and the bearing field. This weakens the building of the radial force.

On the contrary, in the bearingless wound-rotor induction motor the rotor windings have the same number of pole pairs as that of the driving windings. The induced rotor currents are constrained to build a symmetrically distributed field with the same number of pole pairs as that of the driving field. This result enhances the asymmetrical distribution of the air gap field, which results in a larger radial force.

Therefore, the bearingless wound-rotor induction motors can build radial forces more efficiently than the bearingless induction squirrel cage motors. The results of the transient FEM computation depicted in fig. 3 verify this conclusion.

B. *Torque*

The two different rotor structures have also very different influence on the torque. Fig. 4 shows the corresponding transient responses of the torque from the transient FEM computation between these two different rotors. While the bearingless wound-rotor induction motor generates a constant torque independent of the bearing currents, the torque of the bearingless squirrel cage rotor induction motor increases with the bearing currents.

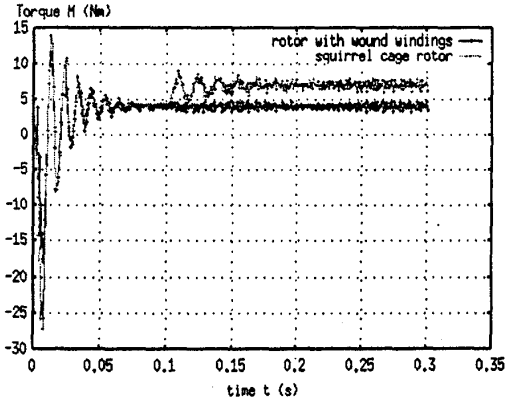

Fig. 4. Transient responses of the torque

The induced rotor currents in the bearingless squirrel cage rotor induction motor will not only generate a 4-pole field but also a 2-pole field. The later can interact with the bearing field to generate another torque component. Then the torque in the bearingless squirrel cage rotor induction motor consists of two parts. One is generated from the driving currents and the other is generated from the bearing currents, which makes the torque dependent of the bearing currents.

On the contrary, in the bearingless wound-rotor induction motor the torque can only be generated from the interaction of the 4-pole driving field and the induced 4-pole rotor currents. The bearing field does not contribute

to the steady torque because the rotor field has different number of pole pairs compared to the bearing field. The results of the transient FEM computation depicted in fig. 4 show the different results of the torque from these two different rotor structures.

V. Control System

A. *Driving Control*

As shown in fig. 4, in the bearingless wound-rotor induction motor the torque is independent of the bearing currents. So the levitation control does not influence the driving control. And we can use the generally used field oriented control for the driving control. Fig. 5 shows the field oriented control for induction motors, which uses the two-axis theory to transform the three phase systems to two phase rotating systems and uses a flux model with a decoupling net to control induction machines like dc machines. The principle and the different machine models of the field oriented control are described in detail in [6]. In the bearingless wound-rotor induction motor we use the field oriented control with constant rotor flux linkage for the driving control, because this method has a short control time constant and a better dynamic response.

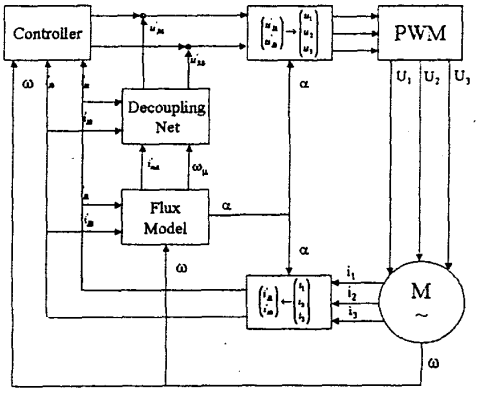

Fig. 5. Field Oriented Control

B. *Levitation Control*

In the proposed bearingless wound-rotor induction motor the radial force is generated from the superposition of the 4-pole field and the 2-pole field. The 2-pole field is built from the bearing currents. Under no-load condition there is only one 4-pole field, i.e. the driving field. But under load condition there are two 4-pole fields, the driving field and the rotor field. The superposition of these two 4-pole fields results in a spatial derivation of the total 4-pole field from no-load position and this derivation varies with the load. If the relative spatial position between the superimposed 4-pole field and the 2-pole field is correspondingly adjusted, the radial force can compensate always the shaft weight.

With this principle a control system is proposed to control the torque and the radial force with one-sided decoupled driving and levitation control. Fig. 6 shows the proposed driving and levitation control system. On the one hand, the levitation control depends on the load of the driving system. The radial force varies with the driving currents and the eccentricity of the rotor. Through a decoupling net and the converter the radial force can be controlled to compensate the shaft weight of the overall driving system and to adjust the rotor to the center of the stator. On the other hand, the levitation control has no influence on the driving control.

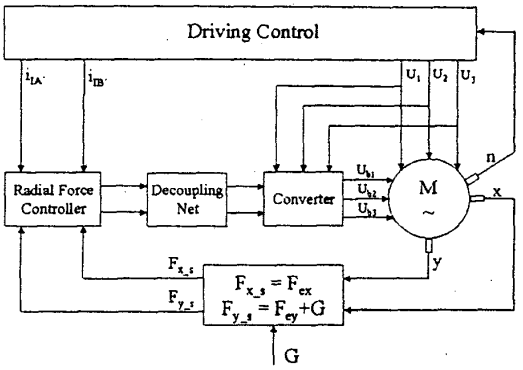

Fig. 6. Driving and Levitation Control System

VI. Conclusion

With the transient finite element method the transient responses of the radial force and the torque are computed for two bearingless induction motors. In comparison to the bearingless squirrel cage induction motor the proposed bearingless wound-rotor induction motor can generate a much larger radial force and a constant torque independent of the bearing currents. A one-sided decoupled driving and levitation control system is proposed to implement the combination of driving and levitation in the bearingless wound-rotor induction motor.

References

[1] A. Chiba, M. A. Rahman and T. Fukao, "Radial force in a bearingless reluctance motor", IEEE Transactions on Magnetics, Vol.27, No.2, pp. 786-790, March 1991.

[2] R. Schöb and J. Bichsel, "Vector control of the bearingless motor" Fourth International Symposium on Magnetic Bearings, ETH Zurich, pp. 327-332, August 1994.

[3] Y. Okada, S. Miyamoto and T. Ohishi, "Levitation and torque control of internal permanent magnet type bearingless motor", IEEE Transactions on Control Systems Technology, Vol.4, No.5, pp. 565-571, September 1996.

[4] K. Ben Yahia, G. Henneberger, "Development of a bearingless induction motor", Proceedings of the Fourth International Conference on Motion and Vibration Control, Zurich, Vol.3, pp. 1083-1087, August 1998.

[5] D. Albertz, G. Arians, G. Henneberger, "Comparison between transient and quasi-stationary calculations of eddy current field problems with moving conductors", COMPEL 19: (2), pp. 173-179, 2000.

[6] G. Henneberger, "Elektrische Maschinen II – Dynamisches Verhalten elektrischer Maschinen, Stromrichterspeisung, Regelverfahren", RWTH Aachen, Germany, February 1994. (in German)